HISTORIC SILK FIBER FRACTURE

by

GAIL ELIZABETH GOODYEAR

B. S., California State University, Chico, 1979

A MASTER'S THESIS

submitted in partial fulfillment of the

requirements for the degree

MASTER OF SCIENCE

Department of Clothing, Textiles and Interior Design

KANSAS STATE UNIVERSITY
Manhattan, Kansas

1981

Approved by:

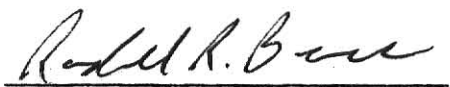

Major Professor

THIS BOOK
CONTAINS
NUMEROUS PAGES
WITH THE ORIGINAL
PRINTING BEING
SKEWED
DIFFERENTLY FROM
THE TOP OF THE
PAGE TO THE
BOTTOM.

THIS IS AS RECEIVED
FROM THE
CUSTOMER.

TABLE OF CONTENTS

ACKNOWLEDGEMENTS

This thesis was completed with the aid and support of a number of people. I would like to express my thanks to Dr. Randy Bresee for his interest in and dedication to my topic and career goals. My appreciation is given to Dr. George Kren, Dr. Elizabeth McCullough, and Dr. Barbara Reagan whose diversity of skills helped attack and complete this problem. Special thanks is given to John Krchma, SEM Laboratory Technician, and Jack Higginbotham, NAA Laboratory Technician, who provided the technical assistance for collecting the data for this study, and the patience and humor necessary to overcome the project's obstacles. Much admiration and affection are given to Dr. Barbara Schreier, Dr. Jane Stolper, and Ms. Suzanne Rosenblatt who contributed the scholastic and social support necessary to survive the traumas of graduate school. Never to be forgotten are Emily Blakeslee, Nancy Ruescher, Karen Patrick, Pat Zbikowski, and the many others whose friendship and companionship made Manhattan wonderful.

A very special thanks is given to my family who contributed to my studies in countless ways. It is unfortunate that my Aunt, Janet Turner, could not see this study completed. She was a loving example I was lucky to have for encouragement. Happily, her impact on my life will never end. I am proud to have for my parents, Hal and Dorothy Goodyear. I am sure my appreciation for their unquestioning and loving support in every direction I have chosen always will show.

I give a big hug to Dave, for he had the patience to endure.

LIST OF FIGURES

LIST OF TABLES

CHAPTER I

INTRODUCTION

Historic costume and textile collections frequently contain items made from silk. The myriad of uses for silk include garments and accessories, ecclesiastical vestments, tapestries, painting canvases, and interior furnishing fabrics. Regardless of the application, silks are subject to debilitating deterioration. The care and preservation of historic silk textiles is a frequent concern of most museum curators because silks chosen to be housed in museums generally are valuable and often irreplaceable. Deterioration in these items often is serious as well as widespread.

Museums seek to house artifacts in an atmosphere conducive to preserving objects in a healthy and usable state. It is not possible, however, to control the museum environment enough to eliminate deterioration of silk textiles. Therefore, these items become more fragile every day and eventually become unusable. The need for a solution to this problem is needed urgently. Since many of the effects of deterioration are visual, records of the appearance of historic silk textiles are being lost. The longer silk deterioration proceeds unchecked, the greater the loss of this irreplaceable resource. The solution to this problem lies in the hands of the researcher.

Little headway has been made in understanding the causes of silk fiber deterioration. While a substantial amount of research involving structure and properties of new silk fibers has been conducted for commercial application, little understanding of the structure and properties of aged silk fibers have been attained. The research reported herein addresses this basic issue. Although this project only represents the first step in understanding the causes of silk deterioration, hopefully it will encourage more work in this area.

The objectives of this study were:

1) To gain insight into the structure and properties of historic silk fibers.
2) To evaluate fiber fracture surface morphology of historic silk fibers.
3) To evaluate the effects of heat and light exposure on the fracture behavior of historic silk fiber morphology.
4) To analyze the elemental chemical compositions of fiber fracture surfaces and whole fabrics from historic silk textiles.

CHAPTER II

REVIEW OF LITERATURE

General Nature of Silk Fibers

Silk is a continuous filament composed of a proteinaceous fibrous biopolymer called fibroin and another proteinaceous non-fibrous biopolymer called sericin (45). Fibroin constitutes the fibrous core of silk fibers, whereas sericin acts as a gummy coating that encapsulates two fibroin filaments. Many animals in the phylum Arthrapoda, classes Insecta and Archnida, extrude these complex filaments (4). Most commercial silk fibers, however, are produced by one animal--the Bombyx mori silkworm (4).

Fibroin and sericin have the general polypeptide repeat unit

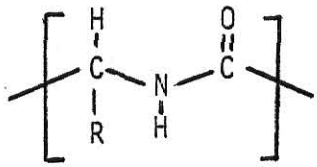

The fibroin polymer is composed of 17 different amino acids, as shown in Table 1, and has a molecular weight between 50,000 and 150,000 (4, 31). Although there is some disagreement among researchers regarding the exact amino acid composition of silk proteins, it generally is agreed that over 80% of the amino acids found in Bombyx mori fibroin are the small, compact peptides: glycine, alanine, and serine (35). In addition, a few of the larger amino acids also are found in appreciable amounts. Tyrosine, for example, comprises about 5% of the fibroin peptides (3). To accomodate both compact and bulky amino acids, it is believed that the fibroin polymer is a block copolymer (3). Blocks of compact amino acids form crystalline segments of fibroin, whereas blocks of bulky amino acids form the amorphous areas. Calculation on the biphasic character of the fibroin polymer, indicates that in a total polymer length of 140 nm, the crystalline and noncrystalline block would be 123 nm and 17 nm, respec-

Table 1

Frequency of Amino Acids in Fibroin

Amino Acid	Amino acid per 100 g. protein (g)
Glycine	43.74
Alanine	28.78
Serine	11.88
Tyrosine	5.07
Valine	2.16
Aspartic acid	1.28
Glutamic acid	1.00
Threonine	0.89
Isoleucine	0.65
Phenylalanine	0.62
Leucine	0.52
Arginine	1.83
Proline	0.35
Lysine	0.63
Histidine	0.53
Tryptophan	0.33
Methionine	0.07
	100.33

SOURCE: Anfinsen, C. B., Jr.; Anson, M. L.; Bailey, K.; and Edsall, J. T., eds. Advances in Protein Chemistry. Vol. 13. New York: Academic Press, Inc., 1958.

tively (31).

X-ray analysis has been used to investigate the morphology of the crystalline unit cell in fibroin. Studies have provided data of the interatomic distances and bond angles in polypeptide chains (31). Further, two principles were developed which explain the possible configuration of the chains. One structural principle which controls the polymer configuration is the coplanarity of the amide linkage that results from overlap of the pi orbitals of the carbonyl moiety with the non-bonding atomic orbital of the nitrogen atom (31).

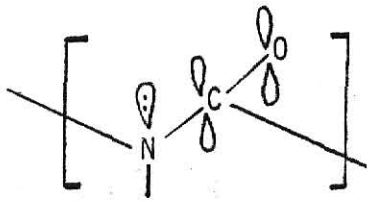

The second structural principle is the formation of nearly the maximum possible number of hydrogen bonds N - H ··· O = C, and the approximate linearity of the atoms forming these hydrogen bonds (31). Therefore, when peptide chains are in an extended form and contain glycine in alternate positions with alanine or serine, the C=O and N-H groups of successive residues project from opposite sides of the chain and are perpendicular to the polymer axis (3, 31). This arrangement enables hydrogen bonds to be formed between adjacent chains laying side by side, forming pleated sheets which may be parallel or antiparallel. The spacial repetition of this arrangement is 6.50Å for parallel sheets and 7.00Å for antiparallel sheets as in silk fibroin (31).

Fibroin fibers have 40-60% orientation of crystalline polypeptide along the fiber axis (3). The birefringence of silk is 0.05. This indicates substantial orientation of all polypeptides of silk (46).

The amino acid composition, orientation, and crystallinity in sericin differs from that of fibroin. Sericin is composed of amino acids which are larger than those contained in fibroin (4). These bulky groups allow for less crystallinity in sericin than in fibroin. The presence of a large number of

acidic and basic amino acids accounts for the gummy nature of sericin. Further, it is somewhat soluble in water whereas fibroin has very low solubility (36). Silk fiber producers generally try to remove the sericin polymer during a degumming process (3). Silk textiles often are weighted with a variety of extraneous salts to restore weight and drapeability lost from degumming (9).

Most natural fibers such as cotton, bast, and animal fibers are cellular and morphologically unlike man-made fibers. Silk, however, is not cellular, but fibrillar and more closely resembles man-made fibers. The shearing forces introduced by the stretch-spinning motion of the silkworm orients the fibrils and forms them into a fiber. Each fibroin fiber has 20 to 30 bundles of highly oriented fibrils (3). Fibrils measure 100Å in diameter and 3500Å long and are grouped into concentric rings (3). The fibrils are held together by an adhering, less organized material called "cuticolina" and, presumably, interfibrillar tie molecules (3, 31).

Fiber Degradation

Changes in the physical and chemical composition of historic textiles are attributed to the treatment and care they receive after fiber formation. The most common effects accompanying silk fiber aging are losses in strength, elongation, and elasticity (39). These factors normally result in a fragile fabric characterized by increased stiffness and brittleness (43).

Polymer aging is a complex process that results from the interplay of a large number of different events which may be classified as either physical or chemical. Physical aging results from the gradual continuation of glass formation and occurs at temperatures below the glass transition temperature (43). Physical aging occurs because amorphous regions in the polymer are not in thermodynamic equilibrium at temperatures below the glass transition tempera-

ture and no additional energy is needed to be supplied for aging to take place (43). Consequently, physical aging may occur in the most gentle environments. Physical aging increases fiber stiffness and brittleness. This process may be reversed, however, by raising the temperature of the polymer substrate to any level higher than the glass transition temperature.

Chemical aging involves the making and breaking of covalent bonds and is essentially irreversible. Energy must be supplied to make or break bonds in chemical aging. The most common energy sources are heat, light, and nonfibrous chemical additives. During the lifetime of a historic textile, it repeatedly is subjected to these three sources of degradation. The most important chemical aging reactions that occur are chain scission and cross-linking. Chain scission results when polymeric skeletal bonds are broken, resulting in lower molecular weight and a broadened molecular weight distribution. Losses in tensile strength, elongation, and elasticity are associated with chain scission. Cross-linking, on the other hand, involves the formation of covalent linkages between two polymer chains. At low reaction levels cross-linking results in increased fiber strength and toughness, while substantially decreased elongation and increased brittleness result at higher reaction levels.

Silk Fiber Degradation

The principle component in degummed silk is fibroin. The glass transition temperature of dry fibroin, as measured by differential scanning colorimetry, is 175°C (32). Consequently, normal storage under non-wet conditions and ambient temperatures of 20 to 25°C place the fiber well below its glass transition temperature, and physical aging will occur. Silk fibers become brittle under storage and at least some of the stiffness found in historic textiles results from physical aging. Because physical aging is a reversible process, this

stiffness may be easily eliminated by exceeding the glass transition temperature of the textiles.

The chemical reactivity of silk has been investigated from predominantly an industrial standpoint, although the decline in commercial interest in the fiber has limited recent research. Knowledge gained from this research may be related to chemical aging of historic silk textiles. However, the multitude of chemical and physical conditions to which a historic textile normally is subjected during its lifetime makes direct application of this research somewhat difficult. Two useful reactions that have been studied, however, are hydrolytic chain scission and oxidative cross-linking (4, 44). Hydrolysis of the peptide linkages in fibroin may occur in boiling water and in steam containing alkalies or mineral acids. These conditions may resemble commercial dyeing and finishing as well as some care treatments. Consequently, the amount of hydrolysis found in historic silk textiles varies and may be substantial in some cases. Silk fibers are susceptible to oxidative degradation. A number of oxidizing agents may induce cross-linking in silk fibroin (4). Since a large number of common substances such as air contain oxidizing agents, the amount of oxidative cross-linking found in historic textiles may vary over a large range and may be substantial in some cases.

Tin has been the most commonly used metallic weighting agent; however, it is not used alone and can be combined with a variety of other agents, such as lead, antimony, aluminum, chromium, manganese, calcium, barium, magnesium, strontium, titanium, zirconium, cerium, didymium, lanthanum, indium, and beryllium (5). Anions commonly used with these metals include chlorides, bromides, sulfates, and nitrates. Weighting procedures based on elements other than tin may be similarly complex chemically. The degree to which a fiber may be weighted is related to the fiber microspaces which are composed of the voids and amorphous areas (37). Different weighting formulations generally require

different methods of application. The diversity of weighting agents and application procedures used throughout history have resulted in an unclear understanding of the effects of specific weighting agents or application procedures on fiber properties.

Silk weighting results in decreased fiber strength and durability (5, 39). It also has been suggested that weighting agents increase silk's susceptibility to damage by sunlight, heat, and perspiration (39). The relative effect of specific weighting agents and application procedures is unknown, however.

Fiber Fracture

Fracture events in polymer materials may be studied at both molecular and morphological levels. Studies utilizing microscopy have examined the morphological details of fiber fracture. The scanning electron microscope (SEM) has facilitated the study of fiber fracture. Most research has been limited to static experiments where the fractographs were taken after the specimen had been fractured outside the microscope.

Hearle (26) has classified fiber failure into ten types. The fracture morphologies of these ten types are illustrated in Figure 1. Type 1 is brittle crack propagation and exhibits a smooth break perpendicular to the fiber axis. This type of fracture is typical of ceramic and elastomeric fibers (16). Type 2 is a cracked opening that forms a V-notch. This controlled ductile crack propagation or tearing is found in nylon and other melt-spun synthetics (11, 13, 15). Type 3 is described as a mushroom shape and is caused by large amounts of plastic deformation. Enough heat is generated to soften the material, which is then flattened into a mushroom shape by snap-back after rupture (14). This type of fracture occurs with nylon fibers under high straining rates. Type 4 occurs from long axial splits which eventually cross the fiber. This pattern

THIS BOOK CONTAINS NUMEROUS PAGES WITH DIAGRAMS THAT ARE CROOKED COMPARED TO THE REST OF THE INFORMATION ON THE PAGE.

THIS IS AS RECEIVED FROM CUSTOMER.

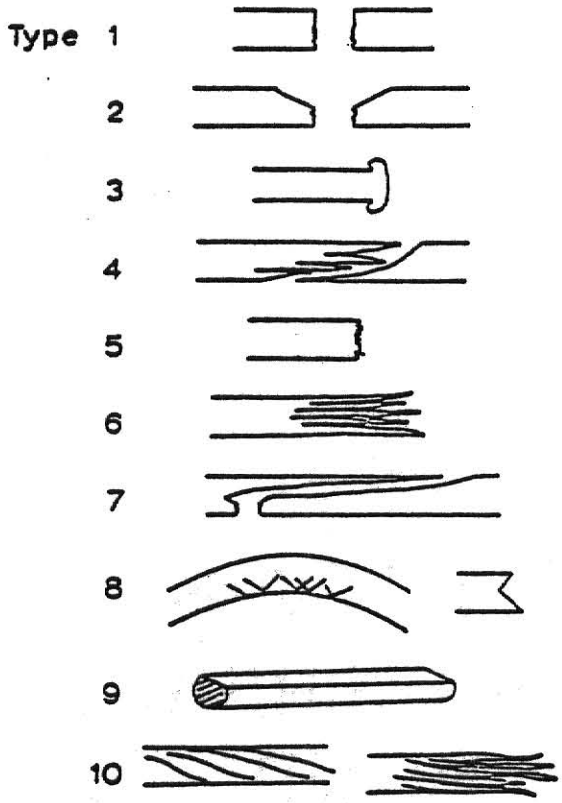

Fig. 1. Schematic Drawings of Hearle's Classification of Fiber Fracture

Source: Hearle, J. W. S.; Buckley, C. P.; and Lomas, B. "Aspects of Fracture of Wool and Hair Fibers." Proceedings 5th International Wool Textile Research Conference. Aechen, Germany: 370-380, 1977.

is more likely to occur if externally induced stresses are present across the axial plane. This type of fracture can occur with highly oriented fibers such as aramids, which resist stresses parallel to the fiber axis, but are susceptible to stress in any nonaxial direction. Type 5 is typified by loss of cohesion between fibrils or other supermolecular structural units. This break is generally found in acrylic and rayon fibers (16). Type 6 occurs when fibrillar units are so weakly linked that they break independently. Type 6 has only been observed with wet cotton fiber fracture studies (12). Type 7 is a long axial split that develops from a surface flaw and leaves a tail on one fractured end which is stripped from the other end (18). This type of failure has been found to occur in aircraft brake parachute cords. Type 8 results from kink bands which eventually split open. The final failure is angular shaped. This failure may occur from flexing over a pin or from wear (13). Type 9 is due to the wearing away of the fiber by surface abrasion until it can no longer support stress and has been observed with several fibers (23). Type 10 is initiated by multiple splits along the fiber. This failure results in a frayed appearance of the fracture and occurs in man-made fibers which have been subjected to biaxial rotation (19, 21, 24, 25).

The fracture behavior of numerous fibers possessing similarities to silk fibers have been examined. Silk is similar to other fibers on a molecular level as well as a morphological level.

Fibers that possess a polyamide composition similar to the structure of silk are wool, nylon 66, and nylon 6. Wool fibers show a tensile failure apparently dominated by its cellular structure. Fracture surface morphology is characterized by breaks perpendicular to the fiber axis (28). Some breaks appear quite smooth while others have a rougher, pebbly surface. Cellular structure is evident in most fractographs (28). Andrew's work supports the importance of the cellular structure in wool fracture (2). He notes, however,

that cuticle cells influence the fracture types while interior cells do not have an obvious effect. Since silk is an extracellular filament, fiber fracture patterns are not dominated by cellular structure as in wool.

Silk possesses a fibrillar morphology and might be expected to display fracture patterns similar to other fibrillar fibers such as wool, nylon, polyester, acrylic, and cotton. Wool exhibits a tensile fatigue fracture typified by long axial splits which join perpendicular cracks across the whole fiber cross-section (28). Long split level breaks are defined by the fibrillar structure of wool. Nylon 6 also possesses a fibrillar morphology. Peterlin suggested that the microfibril ends located mainly in the outer boundary of the fibrils represent an interruption in the axial connection of tie molecules (34). Therefore, these areas would be susceptible to microcrack formation under tensile stress. The fiber would fail when one of the cracks reached critical dimensions. Brecht, et al. support Peterlin's suggestion, adding that molecular associations must be considered in addition to polymer chain strength (6). Further, the nylon 6 fracture pattern shows characteristics similar to that of polyester, although polyester fibers have a rough area at the edge of the fiber that is more pronounced (27).

Acrylic fibers have been found to have tensile fracture patterns exhibiting a granular surface (7). This pattern suggests the separate failure of fibrillar units. Acrylic fibers contrast other melt-spun synthetic fibers which show a fracture pattern based mainly on crack development. The fibrillar breakage characteristics, however, are similar to those observed in cotton, rayon, and wool fibers.

Cotton fracture is based on interfibrillar cohesion which is dependent upon treatment variations and other characteristics (29). Cotton fibers broken in water have long fibrillar splits, while those broken dry are shorter (29). These variations are due to different amounts of interfibrillar bonding. Cotton

fibers which break at reversals display long fibrillar splitting, while those broken between reversals exhibit shorter splitting (29). This difference may be attributed to crack development which can occur near the reversals. Consequently, it seems that fibrils break more independently in the absence of physical heterogeneities that may encourage catastrophic failure by crack development.

Since silk is a natural fiber possessing surface flaws and interval voids, fracture patterns which are dominated by the presence of these heterogeneities in the fiber should be observed. The same can be said for other natural fibers such as wool. The fracture of wool under flextural fatigue occurs by formation of a flat surface which then leads to failure of the fiber similar to split level tensile breaks. Makinson observed that cracks generally are located at deformed regions of the wool fiber, which suggests that they are initiated by local concentrations of stress (33). Andrews supports this idea with evidence that fracture is propagated by local flaws (2).

The failure mechanism of nylon 66 stressed under tension is dominated by ductile crack growth (10, 11, 16, 18). Hearle found that the mechanism may be altered under cyclic loading conditions (8). These conditions allow stress induced crystallization to occur which arrests the strain in small faults on the fiber surface and deflects the crack from its original axis.

The effect of heat treatments on fracture of polyamide fibers has been investigated (22). Studies have shown, for example, that heat treatments alter the normal ductile crack growth fracture behavior of nylon 66. Heat degraded fibers exhibited a reduction in strength and elongation and an increase in brittleness. At 200°C nylon 66 fibers exhibited a rough surface fracture, while at 225°C the fibers show a smooth fracture surface (22). This indicates a change in the ductile character of the unheated fiber to a morphology displaying less interfibrillar cohesion and finally to a completely embrittled fiber

matrix breaking along one fracture plane.

The effect of photochemical degradation on fiber fracture has been examined for nylon 66 fibers (20). The normal ductile crack growth fracture behavior of nylon 66 was modified by photochemical degradation. In delustered fibers, it was found that light causes the polymer near the titanium dioxide particles to oxidize and create voids from which breaks would be initiated (27). The fiber appeared badly cavitated and seemed to have broken in a brittle manner. It also is well known that fracture can be initiated by surface dirt and flaws (47). And it would be expected that breaks would be able to start at the many cavitated areas.

CHAPTER III

PROCEDURE

Twenty-five silk fabrics dating between 1880 and 1980 were subjected to tensile stress to determine the effects of chronological age, chemical composition, heat and light exposure on the fracture surface morphology of fibers. Fabric specimens were broken using a Scott CRE tensile tester and then evaluated with a scanning electron microscope (SEM) to characterize the types of fiber fracture which occurred. Chemical composition of the silk fabrics was assessed using energy dispersive x-ray and neutron activation analyses (NAA).

Sample Selection

Twenty-four fabric samples were obtained from the textile collections at Kansas State University; California State University, Chico; and the Fort Riley Military Museum (see Table 2). Curators from participating museums were requested to submit 5 x 5 cm samples of plain weave, silk lining fabrics for the study. Sample selection was based on age, fabric construction characteristics, size, and fiber content. A sample of degummed silk crepe (Style #601, Testfabrics, Inc.) was used as the twenty-fifth sample (specimen number 15). An additional sample was taken from this fabric and subjected to heat (specimen number 26) and to accelerated light (specimen numbers 27 and 28).

Sample Preparation

To remove surface dirt and oils, each silk sample was agitated gently in perchloroethylene for 2 minutes at 25°C, conditioned at 21 $\pm$ 1°C and 65 $\pm$ 2% RH for 24 hours, agitated in a 0.05% aqueous solution of nonionic surfactant

Table 2

Historic Data for Silk Fabrics

Sample Number	Date	Color
1	1904	Black
2	1885	Black
3	1952	Black
4	1964	Blue & White
5	1909-10	Lavender
6	1880	Off White
7	1904	Off White
8	1904	Pink
9	1903-10	Black
10	1910	White
11	1900	Black & Blue
12	1973	Pink
13	1905	White
14	1898	Off White
15	1980	White
16	1937	Brown
17	1928	Salmon
18	1900-06	Grey
19	1900-10	Off White
20	1940	Off White
21	1929	Off White
22	1914	Grey
23	1913	White
24	1905	Off White
25	1930	Black
26	1980	White
27	1980	White
28	1980	White

(Merpol LF-H) at 25°C for 2 minutes, rinsed successively in 10 distilled/deionized water baths at 25°C, dried, and then reconditioned for three days prior to tensile fracture.

Tensile Fracture

Specimens measuring 1 x 5 cm with the long dimension parallel to the warp were prepared from the 25 silk fabrics. Adhesive tape was applied to ends of the specimens to facilitate placing them between the clamps of the Scott CRE tensile testing machine. Because of the limited specimen size, the distance between the clamps was 1 cm at the start of the test. The general procedures in ANSI/ASTM D1682-64, Breaking Load and Elongation of Textile Fabrics (46), were followed using a constant traverse speed of 30.5 $\pm$ 1 cm per minute.

Heat Exposure

Samples of degummed silk crepe (Style #601, Testfabrics, Inc.), measuring 30.5 x 30.5 cm, were heated for 6 hours at 60 $\pm$ 2°C in a Precision Scientific laboratory convection oven. To assess the fracture patterns produced on the heat-treated silk during tensile stress, 1 x 5 cm specimens were cut from the center of the silk fabrics after heating, conditioned, and then subjected to tensile forces by using the procedure described above.

Accelerated Light Exposure

The effect of accelerated light exposure on silk fiber fracture patterns was evaluated after exposing 26.5 x 18 cm specimens of the degummed silk crepe (Style #601, Testfabrics, Inc.) to carbon arc radiation for 320 AATCC Fading Units. The procedures used for light exposure were those specified in AATCC

Test Method 111C-1975, Weather Resistance: Carbon Arc Lamp Exposure Without Wetting (46). Specimens were mounted in open back metal frames with the warp in the vertical direction and exposed to continuous light in an Atlas carbon arc Weather-Ometer, Model 18 WR. The black panel temperature and relative humidity during exposure were 37.8 $\pm$ 6°C and 80 $\pm$ 5% RH.

AATCC Blue Wool Lightfastness Standards were used to determine the number of AATCC Fading Units to which the silk specimens were exposed, following the procedure specified in AATCC Test Method 16-1978, Colorfastness to Light: General Method (46). The silk test specimens were exposed to carbon arc radiation until the L-8 AATCC Blue Wool Standard exhibited a step 4 color change on the AATCC Gray Scale for Color Change. This was equivalent to 320 AATCC Fading Units.

Scanning Electron Microscope Analysis

Fractured ends of each silk specimen were analyzed with the scanning electron microscope (SEM) at Kansas State University. The SEM analysis was comprised of two parts. The first part used the energy dispersive x-ray analyzer of the SEM to determine the elemental composition of fiber fracture surfaces; the second part consisted of recording photomicrographs of fiber fracture surfaces. The photomicrographs aided in classification and identification of fracture types.

Fractured silk fibers were mounted for SEM analysis using the following method. Unbroken ends of short lengths of several fractured fibers in a specimen were embedded vertically in Pelco carbon paste on a SEM specimen holder by using an optical microscope and tweezers. Approximately 20 fibers from each fractured fabric were mounted. The specimens were then evaporatively-coated with carbon in a Kinney Vaccum Evaporator. The carbon coating did not inter-

fere with the energy dispersive x-ray analysis, although resolution and contrast of SEM photomicrographs from these specimens were poor.

Three fractured ends morphologically representative of the 20 mounted fibers were chosen for SEM analysis. A total of 25 fabrics yielded 75 fractured ends that were semi-quantitatively analyzed by energy dispersive x-ray analysis using an Ortex Detector with a Norland multichannel analyzer. This was accomplished by focusing a beam of electrons on the center of the fractured fiber end. The emitted x-rays were collected for 80 seconds and recorded with a strip chart recorder. The fracture end of each fiber was photographed, and rotation and tilt angles were recorded so the same fiber end could be found again for the final photomicrograph.

The specimens were then evaporatively coated with a gold-palladium alloy (60/40). This metal coating provides an excellent photomicrograph by increasing resolution and contrast. Previously taken photomicrographs and recorded tilt and rotation angles were used to find the fractured fiber end which had been analyzed elementally. A final photomicrograph of each of the 75 fibers was recorded at 1000-4000X.

Neutron Activation Analysis

This analysis consisted of inserting the specimens into a TRIGA Mark II nuclear reactor, removing the resulting radioactive specimens, and analyzing the gamma ray spectrum using a Germanium-Lithium drifted solid state detector connected to a multichannel analyzer. The gamma ray spectrum provided semi-quantitative information concerning the elemental composition of the sample.

Twenty-five silk specimens and one reference standard were analyzed. Each sample was placed inside a 0.2 ml polyethylene vial which previously had been cleaned with methanol to remove NaCl contamination. The mass of each silk

specimen was then determined. A piece of iron wire was wrapped around each vial and the wire mass was determined. Each vial was then sealed by melting its cap to the sides of the vial. Each vial, once again, was washed with methanol.

Each specimen was inserted into the reactor 3 times. The first and second insertions were for 3 minutes at a reactor power level of 100 kw. The last insertion was for 45 minutes at 225 kw. After each neutron exposure, specimens were carried to the NAA laboratory and laid in the center of the detector. The gamma ray spectra for each specimen were collected for 400 seconds and then recorded in magnetic tape. The spectra of each iron wire were collected for 300 seconds and then recorded on magnetic tape. The decay times, representing the time of specimen removal from the reactor to initiation of gamma ray collection, were determined by using the iron wire data. Since the isotope emits a unique gamma ray spectrum, the elemental composition of the specimens was determined by identifying characteristic peak energies in each spectrum. The isotopic composition of the specimens was determined from this spectra. The mass of each isotope present in the specimens was evaluated by using a WATFIV computer program. The program calculated the mass of each isotope based on decay times of the iron wires, the 25 silk specimens and the reference specimen, the mass of the wires and specimens, and the peak areas.

CHAPTER IV

RESULTS AND DISCUSSION

Fiber Fracture Morphology

The fracture surfaces of the broken silk fibers were classified according to Hearle's system of fiber fracture morphology (26). Most fractured ends observed in this study fit this system. However, some of the fractured surfaces could not be classified as any of the ten types used by Hearle. The fracture types assigned to the silk specimens evaluated in this study are presented in Table 3.

Fracture types 1, 3, 4, 6, and 10 were not found in the historic silk specimens or the degummed silk crepe specimens after they were subjected to a tensile load to the point of break. Type 1 fracture, which results from brittle crack propagation along one plane perpendicular to the fiber axis, was not expected. This type of fracture has only been found in ceramic and elastomeric fibers. These fibers possess little or no sizeable crystalline morphology and are, more or less, structurally homogenous in the size range characteristic of supramolecular structures. Consequently, the fiber acts as a single unit and fracture occurs along one fault line. On the other hand, silk fibroin possesses a fibrillar morphology and is structurally heterogeneous in the supramolecular size range. Fracture of silk fibers would be expected to follow lines of supramolecular structure instead of following a single fault line. However, severe fibrillar degradation might result in sufficient homogeneity to allow type 1 brittle fracture to occur. The lack of type 1 fractures in this study indicates that supramolecular structure in every sample was not degraded severely enough to cause fracture along a single fault line.

The absence of type 3 fractures was expected. This fracture type has

Table 3

Fracture Types in Silk Fabrics

Sample No.	Fracture Type											
	1	2	3	4	5	6	7	8	9	10	11	12
1					1							
							2					
					3							
2							1					
								2				
							3					
3		1										
					2							
							3					
4					1							
		2										
					3							
5								1				
											2	
					3							
6					1							
					2							
					3							
7					1							
		2										
		3										
8							1					
												2
							3					
9		1										
												2
							3					
10								1				
					2							
					3							
11							1					
								2				
					3							
12					1							
								2				
					3							
13		1										
							2					
								3				
14					1							
					2							
					3							
15		1										
							2					
							3					

(Table 3 cont'd)

Sample No.	Fracture Type											
	1	2	3	4	5	6	7	8	9	10	11	12
16					1 2 3							
17							1 3					2
18		3			2							1
19					1 2 3							
20					1 2 3							
21							1 2 3					
22		2			3		1					
23		1			2						3	
24								1 2				3
25		2										1 3
26					1 2 3							
27							1 2 3					
28							1 3				2	

NOTE: Fracture types were classified according to Hearle's fiber fracture system. The three fractured fiber ends of each sample were numbered 1, 2, and 3 and tabled as to fracture type.

been observed only with nylon fibers fractured at very high stress rates where heat buildup is sufficient to melt the polymer material. The tensile loading rate in this study was very low and little heat build up occurred.

No fractured fiber ends in this study were found to exhibit a type 4 fracture. This type of fracture is observed when discontinuities along planes perpendicular to the fiber axis are present in fibers which are highly oriented parallel to the fiber axis and are very weak perpendicular to the fiber axis. Para substituted aromatic polyamides typically display type 4 fracture behavior. Since fibril orientation in silk fibroin is not nearly as high as in these polyamides, it is not surprising to find an absence of type 4 fractures in the samples examined in this study.

No fractured ends were classified as type 6 in this study. This fracture type is observed when fibrillar units are so weakly united they break independently. This type of fracture has only been observed with wet cotton fibers. The absence of type 6 fractures in this study indicates that interfibrillar cohesion in historic silk is greater than that of wet cotton fibers.

Type 9 fractures were not found in this study. This fracture type is characterized by a wearing away of the sides of the fiber by surface abrasion. This study examined tensile fracture and not surface abrasion.

We did not observe type 10 fractures which are characterized by multiple splitting. Type 10 fibers are broken by biaxial rotation. Since this study involved a tensile break, this fracture type would not be expected.

According to Hearle's classification system, fracture types 2, 5, 7, and 8 were observed in the silk samples examined in this study. Two other fracture types were observed, voids and multiphasic fractures, which were numbered 11 and 12 respectively, for this project.

Type 2 fractures were found in 9 or 12% of the fractured ends examined.

Figures 2 and 3 show this fracture type which is typified by a controlled ductile crack propagation with the crack opening to form a V-notch. Finally the crack becomes catastrophic. Type 2 fractures have been observed with several melt-spun synthetic fibers including nylon. This fracture behavior indicates the presence of ductile polymer material. Since none of the fibers examined in this study exhibited brittle type 1 fracture or the plastic flow of type 3 fracture, the presence of somewhat ductile type 2 fractures were expected.

Type 5 fractures were the most commonly found fracture pattern in this study. Thirty-three fractured ends or 44% of the fractured specimens exhibited this behavior. This type of fiber fracture results from transverse discontinuities among fibrils or other structural units which do not allow direct crack propagation, but are able to trigger breaks in neighboring units. This fracture type is visually identified by a granular surface, representing definition of individual structural units. This fracture is shown in Figures 4-7. The uniformly, pebbled fracture surface in Figure 4 indicates a uniform, internal fiber structure. On the other hand, the presence of more than one morphological unit on the fracture surface in Figure 5 indicates nonuniform internal fiber structure. Figure 6 shows a split level type 5 break, resulting from crack propagation occurring in two planes.

A type 5 fracture might commonly be expected in historic silk fabrics as structural discontinuities are introduced in fibrils during aging. This view is supported by the heat treated specimens of degummed silk crepe which suffered a 85% loss in breaking strength due to the treatment. The fracture pattern is shown in Figure 7. The heat treated specimens only exhibited type 5 fractures, whereas the nonheat treated specimens exhibited fracture types 7 and 8. Thus, it appears that heat exposure during aging introduces structur-

THIS BOOK CONTAINS SEVERAL DOCUMENTS THAT ARE OF POOR QUALITY DUE TO BEING A PHOTOCOPY OF A PHOTO.

THIS IS AS RECEIVED FROM CUSTOMER.

THIS BOOK CONTAINS NUMEROUS PICTURES THAT ARE ATTACHED TO DOCUMENTS CROOKED.

THIS IS AS RECEIVED FROM CUSTOMER.

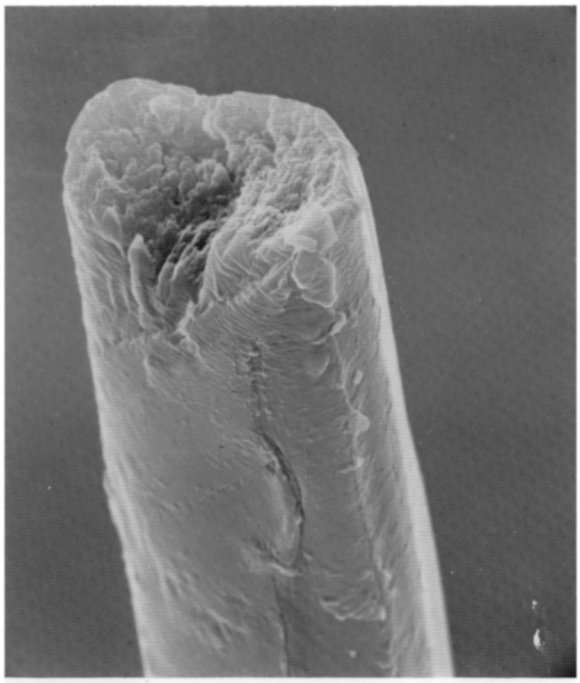

Fig. 2. Type 2 Fracture (X4000)

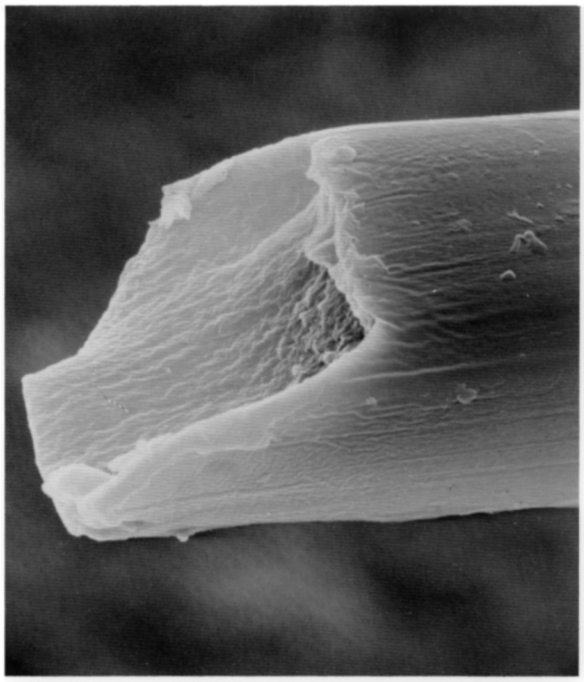

Fig. 3. Type 2 Fracture (x4000)

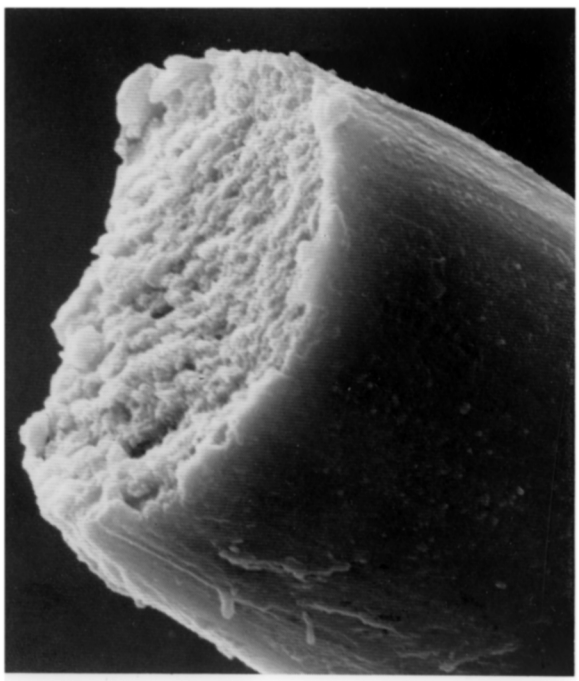

Fig. 4. Type 5 Fracture (X4000)

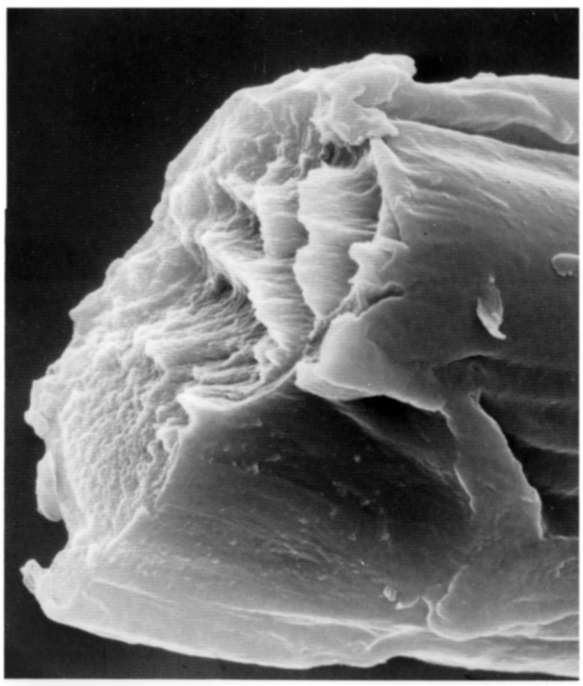

Fig. 5. Type 5 Fracture (X4000)

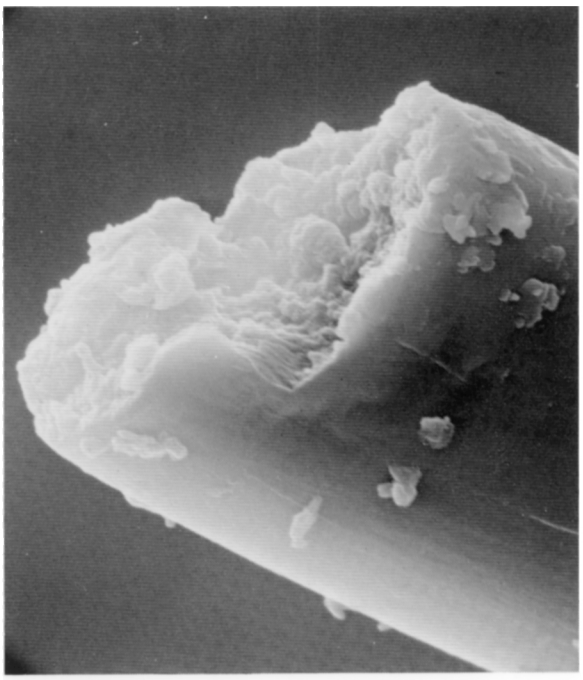

Fig. 6. Type 5 Fracture (X4000)

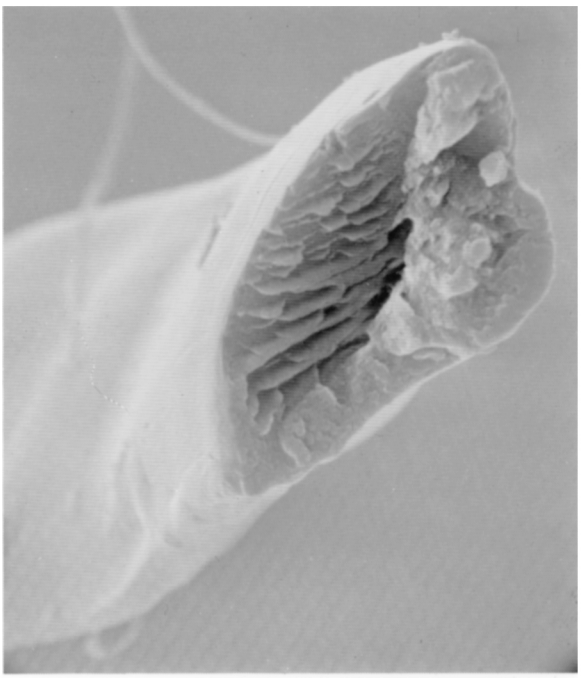

Fig. 7. Type 5 Fracture (X4000)
(heat exposed sample)

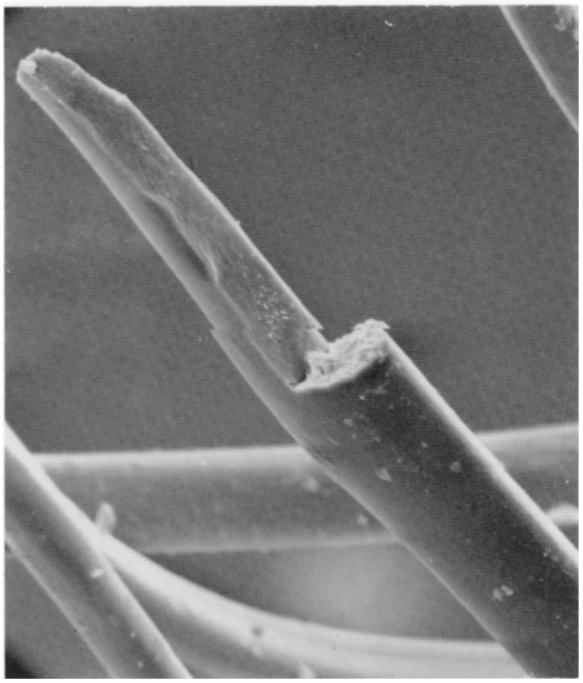

Fig. 8. Type 7 Fracture (X1000)

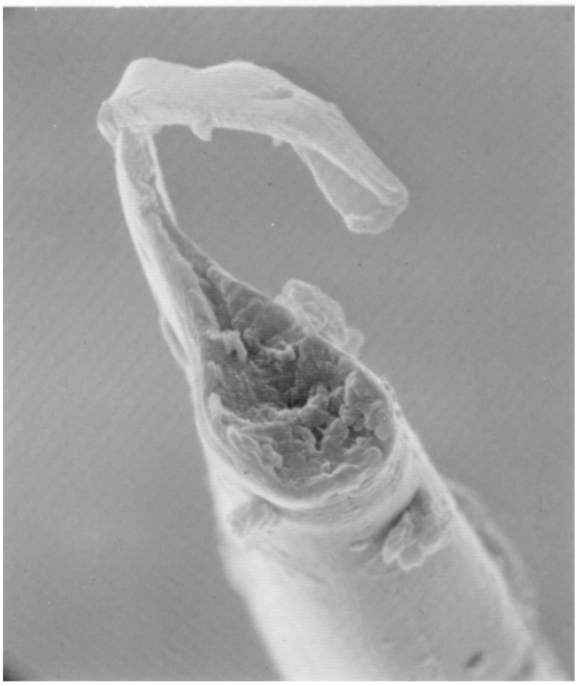

Fig. 9. Type 7 Fracture (X4000)

al heterogeneities into the fibers that alter their fracture behavior.

Type 7 fractures also were found in relatively high numbers in this study. Twenty-two or 29% of the fractured ends were classified as type 7 breaks. Type 7 fractured ends may be seen in Figures 8 and 9. This fracture type is characterized by a long axial split which develops from a surface flaw and leaves a tail on one fractured end and stripped off at the other fractured end. Since silk is a natural solution spun fiber with frequent structural flaws one would expect to observe this pattern frequently.

The fractured fibers of the degummed silk crepe which was exposed to light exhibited predominantly type 7 breaks. These fabrics suffered a 92% loss in breaking strength after being exposed to 320 AATCC Fading Units under carbon arc radiation. The predominance of this fracture type could be attributed to the occurrence of surface flaws in these light exposed fabric samples.

Type 8 fractures were found in 8 or 11% of the specimens evaluated. A type 8 fracture is typified by a split which has opened up from a kink band. A typical type 8 fractured end found in this study is pictured in Figure 10. These fractures probably were seen because fabrics instead of fibers or yarns were broken in this study. That is, fabric interlacings cause fibers to be stressed over other fibers instead of along the fiber axes.

Fracture types other than those discussed by Hearle were found in this study. They were classified as types 11 and 12. Type 11 breaks were attributed to voids which were found in 3 or 4% of the specimens. This type is shown in Figure 11. These voids could be caused by any disruption of the polymer when extruded by the silkworm. The presence of a void would cause stress to be concentrated in the polymer surrounding the void so fracture at the void location is likely.

Type 12 breaks were found in 7 ends or 9% of the specimens examined. This

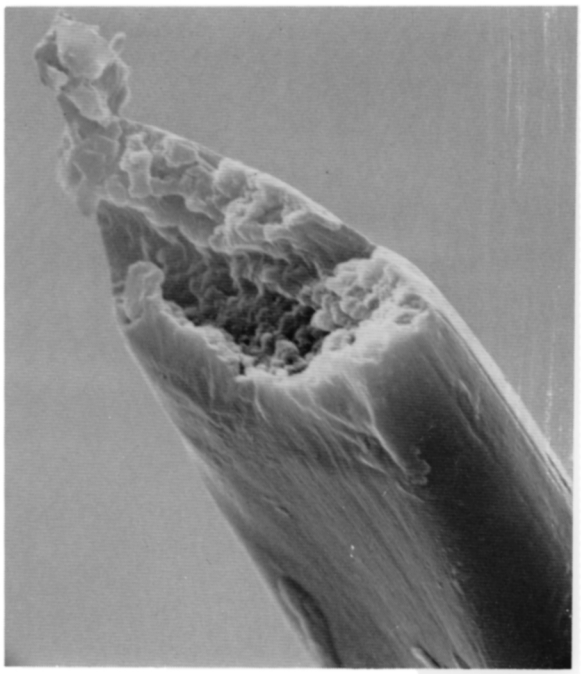

Fig. 10. Type 8 Fracture (X4000)

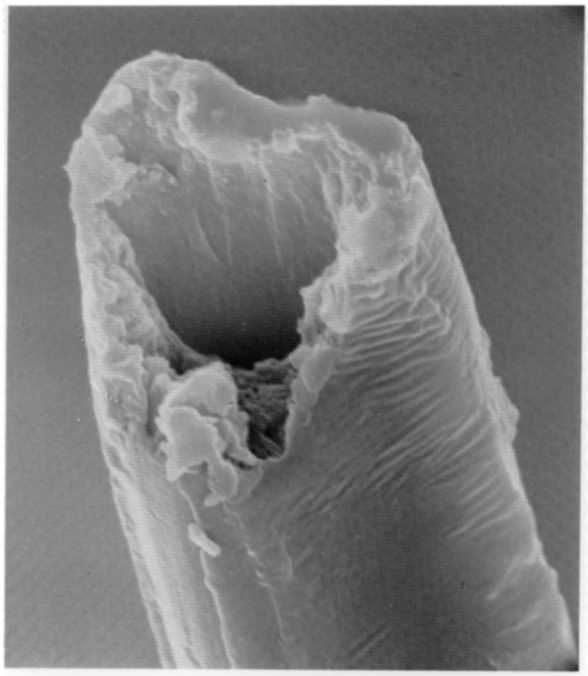

Fig. 11. Type 11 Fracture (X4000)

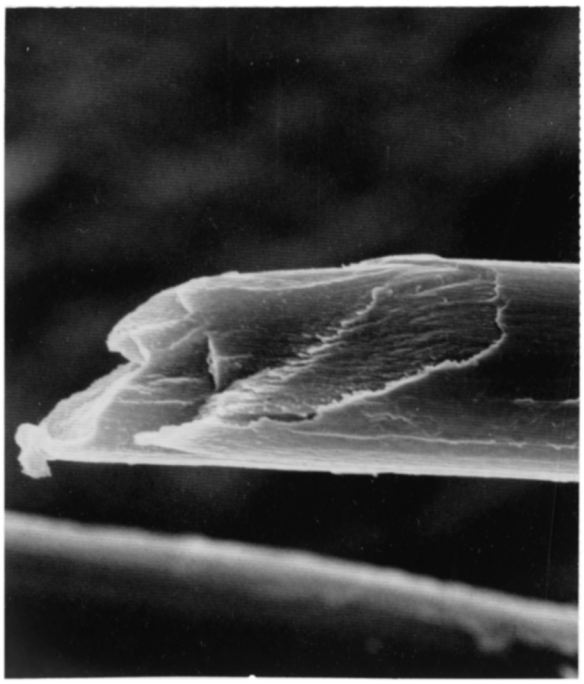

Fig. 12. Type 12 Fracture (X3000)

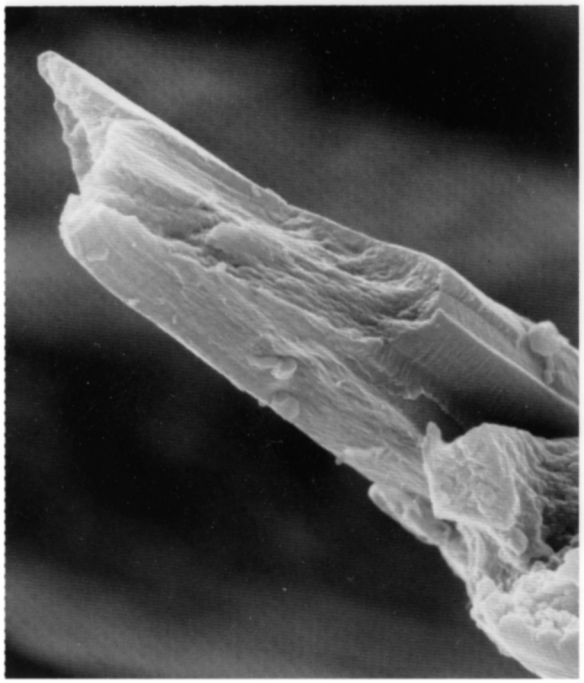

Fig. 13. Type 12 Fracture (X4000)

type of fracture is a result of a number of influences on the fiber as it breaks Brittleness, loss of fibrillar cohesion, and external and internal flaws may have caused multiphasic breaks which were found in many of silk specimens. The characteristic multiphasic breaks observed in this study are pictured in Figures 12 and 13.

Energy Dispersive X-ray and Neutron Activation Analyses

Surfaces of the fractured ends of the 25 silk fabrics were subjected to energy dispersive x-ray analysis to determine the elemental chemical composition of these areas. Additional specimens from each fabric were analyzed by neutron activation analysis which provided information about the elemental chemical composition of the whole fabrics. The elemental composition data of the fiber fracture surfaces and of the whole fabrics were compared to determine the distribution of chemical additives throughout the fibers. It was hoped that by evaluating the homogeneity and heterogeneity of the chemical additives, the role of these chemicals in silk fiber fracture could be more thoroughly understood.

Energy dispersive x-ray analysis is capable of detecting elements heavier than sodium. Silicon was present in all specimens evaluated. Other elements found in many of the specimens were chlorine in 29%, sulfur in 16%, tin in 15%, and phosphorus in 12%. Elements were found in fewer specimens. These included calcium in 4%; potassium in 4%; iron in 3%; and antimony, lead, niobium, and zinc in 1% of the samples.

Several of the elements identified by energy dispersive x-ray analysis could not be detected, however, by neutron activation analysis, and vice versa. Based on the neutron activation data all the specimens contained silicon, 88% contained tin, and 19% contained iron. Other isotopes detected in a smaller number of the specimens were bromine in 9%, magnesium and copper in 5%, and indium and

antimony in 3%.

The energy dispersive x-ray analysis data was assigned a numerical rating based on relative element concentration (see table 4). This numerical rating was then ranked according to concentration for each element (see tables 5, 6, and 7).

The neutron activation data was evaluated by calculating the mass ratio of each spectrum relative to a standard of known elemental concentration. The mass ratio values were then ranked according to magnitudes (see tables 8 through 15).

The two ranked, relative values were then compared to determine if the fracture surface concentrations (energy dispersive x-ray analysis) were consistent with concentrations in the total fiber specimen (neutron activation analysis). This comparison showed that indium, antimony, magnesium, iron, and silicon were present in about the same relative concentrations in both fracture surface and total fiber. It is reasonable to assume that these elements were distributed uniformly throughout the fibers. From the data of this study it cannot be determined whether these elements may promote fiber fracture.

Fracture types dependent on the presence of heterogeneities would be expected to occur more frequently in specimens that showed a difference in concentration between fracture surfaces and whole fibers. This study showed that tin was not uniformly distributed throughout the fiber in 33% of the fibers containing tin (specimens 16, 18, and 19). Consequently, the fracture behavior of these fibers might be dependent on heterogeneities resulting from a non-uniform distribution of tin throughout the fiber. Type 5 fractures were identified for 78% of the specimens which did not have tin distributed uniformly throughout the fiber (samples 16, 18, and 19), compared to 40% of the specimens which had tin uniformly distributed in the fibers. A type 5 fracture is based on heterogeneities in the fiber. It may be that the heterogeneities in these fibers was caused

Table 4

Energy Dispersive X-ray Analysis

	Element																			
	Na	Mg	Al	Si	P	S	Cl	K	Ca	Mn	$Fe_{K\alpha}$	$Fe_{K\alpha}$	Sn_L	Sn_L	Sn	Sb	Pb	Nb	Zn	In
	Fiber Number																			
Sample #	1 2 3	1 2 3	1 2 3	1 2 3	1 2 3	1 2 3	1 2 3	1 2 3	1 2 3	1 2 3	1 2 3	1 2 3	1 2 3	1 2 3	1 2 3	1 2 3	1 2 3	1 2 3	1 2 3	1 2 3
1				3 3 3	4 4 3	4 4 3	4 4 3						5 5 5	3 3 3						
2				4 4 5			- - 1						5 5 3	3 4 2	2 2 1					
3	- 1 -			4 - -		4 4 4	3 - 3	1 - -	1 - -											
4		1 - -		5 4 4		- 3 4	1 3 5		- 2 -											
5				5 5 5	1 1 1		1 1 1						3 3 3	2 2 2	- 1 1	- 1 1				
6			4 - 3	3 4 4			3 3 3	3 2 2	- 1 -											
7	1 - 1	1 1 -		5 5 5	1 1 1	- - 1	1 1 1						5 3 3	3 2 2	- 1 1					
8	- 1 -			- 3 -	3 4 3	- 2 3	- 2 3						5 5 5	4 3 3				3 4 3		
9	3 3 3			5 5 5			5 5 5				3 3 3		4 3 3	3 3 3						
10				5 5 5	1 1 1	1 1 1	1 1 1						3 2 3	1 1 1						
11	1 - -			4 5 5		3 3 -	- 5 4		3 2 3		4 4 4	1 1 1								2 2 2
12				4 4 4			- - 3													
13				5 4 4																
14	1 1 2			5 5 5			2 2 1						4 4 4	3 3 3						
15				4 4 4																
16	1 1 1			5 5 5	2 2 2	4 4 3	1 1 1						2 2 2	1 1 1			4 3 3			
17				4 3 4	- 4 -	- - 4	5 - 3	4 - -	- 2 -										4 - -	
18				5 5 5	1 1 1								2 2 2	1 1 1						
19				5 5 5	1 1 1		1 1 1						2 2 2	1 1 1						
20				5 5 5		3 3 3	3 3 3													
21				5 4 4		- 3 -	3 2 3													
22				5 5 5			- - 3													
23				5 5 5		3 - -	2 3 3													
24				5 5 5			- - 3													
25			5 5 4	5 4 5		4 3 5	- 2 3													

NOTE: Each fiber was ranked on relative elemental concentration. The spectral peaks were assigned values as follows: 1 = peak height from 1-2 cm, 2 = peak height greater than 2 cm and less than 7 cm, 3 = peak height greater than 7 cm and less than 10 cm, 4 = peak height greater than 10 cm and less than 5 cm, and 5 = peak height greater than 15 cm.

by the nonuniform distribution of tin.

Table 5

Iron: Energy Dispersive X-ray Analysis

Sample Number	Rank	Average Rating
11	1	4
9	2	3

Table 6

Tin: Energy Dispersive X-ray Analysis

Sample Number	Rank	Average Rating
1	1	5
8	1	5
2	2	4.3
14	3	4
7	4	3.6
9	5	3.3
5	6	3
16	7	2
18	7	2
19	7	2

Table 7

Silicon: Energy Dispersive X-ray Analysis

Sample Number	Rank	Average Rating
5	1	5
7	1	5
9	1	5
10	1	5
14	1	5
16	1	5
18	1	5
19	1	5
20	1	5
22	1	5
23	1	5
24	1	5
11	2	4.6
21	2	4.6
25	2	4.6
2	3	4.3
4	3	4.3
13	3	4.3
15	4	4
6	5	3.6
17	5	3.6
1	6	3
3	7	1.3

Table 8

Indium: Neutron Activation Analysis

Sample Number	Rank	Mass Ratio
Standard	0	(.10000E 01)
18	1	(.53535E 01)
19	2	(.77084E 01)

Table 9

Copper: Neutron Activation Analysis

Sample Number	Rank	Mass Ratio
Standard	0	(.10000E 01)
18	1	(.12716E 01)
3	2	(.45398E -01)
8	3	(.36282E -01)
5	4	(.35945E -01)

Table 10

Antimony: Neutron Activation Analysis

Sample Number	Rank	Mass Ratio
Standard	0	(.10000E 01)
10	1	(.18736E -02)
5	2	(.15936E -02)

Table 11

Magnesium: Neutron Activation Analysis

Sample Number	Rank	Mass Ratio
Standard	0	(.10000E 01)
14	1	(.19889E 01)
7	2	(.10580E 00)
3	3	(.27928E -01)

Table 12

Bromine: Neutron Activation Analysis

Sample Number	Rank	Mass Ratio
Standard	0	(.10000E 01)
4	1	(.81276E -02)
25	2	(.12592E -02)
22	3	(.56426E -02)
23	4	(.40314E -02)
19	5	(.31465E -03)
21	6	(.15218E -03)
24	7	(.13732E -03)

Table 13

Iron: Neutron Activation Analysis

Sample Number	Rank	Mass Ratio
Standard	0	(.10000E 01)
16	1	(.25978E 02)
9	2	(.19186E 02)
8	3	(.14718E 02)
1	4	(.13335E 02)
5	5	(.60196E 01)
11	6	(.39593E 01)
12	7	(.22449E 01)
22	8	(.21753E 01)
19	9	(.17673E 01)
23	10	(.14496E 01)
24	11	(.83126E 01)
25	12	(.51494E 01)
2	13	(.32126E 00)
6	14	(.22546E 00)

Table 14

Tin: Neutron Activation Analysis

Sample Number	Rank	Mass Ratio
Standard	0	(.10000E 01)
14	1	(.18808E 03)
18	2	(.14284E 03)
16	3	(.95897E 02)
8	4	(.17109E 02)
17	5	(.15346E 02)
10	6	(.14062E 02)
5	7	(.11539E 02)
2	8	(.11526E 02)
7	9	(.80868E 01)
1	10	(.76635E 01)
9	11	(.66270E 01)
17	12	(.10295E 01)
11	13	(.24345E 00)
15	14	(.12592E 00)
25	15	(.98824E -01)
4	16	(.86289E -01)
6	17	(.35837E -01)
22	18	(.24595E -01)
23	19	(.21345E -01)
21	20	(.18066E -01)
24	21	(.16452E -01)
20	22	(.11614E -01)

Table 15

Silicon: Neutron Activation Analysis

Sample Number	Rank	Mass Ratio
Standard	0	(.10000E 01)
16	1	(.12902E 00)
19	2	(.12539E 00)
18	3	(.91436E -01)
7	4	(.89225E -01)
10	5	(.83430E -01)
8	6	(.83316E -01)
5	7	(.74057E -01)
17	8	(.57588E -01)
14	9	(.56524E -01)
1	10	(.37036E -01)
25	11	(.33532E -01)
6	12	(.29943E -01)
23	13	(.27040E -01)
20	14	(.22373E -01)
9	15	(.22317E -01)
13	16	(.21611E -01)
3	17	(.18077E -01)
4	18	(.16643E -01)
11	19	(.14604E -01)
22	20	(.13054E -01)
21	21	(.13050E -01)
24	22	(.11964E -01)
15	23	(.11462E -01)
12	24	(.10032E -01)
2	25	(.99676E -02)

CHAPTER V

SUMMARY AND CONCLUSIONS

Twenty-five silk samples dating between 1880 and 1980 were subjected to tensile stress to determine the effects of chronological age, elemental chemical composition, heat and light exposure on the fracture surface morphology of silk fibers. Information on fiber fracture morphology was obtained from scanning electron photomicrographs. Elemental composition of the silk fibers was obtained by energy dispersive x-ray and neutron activation analyses.

No correlation between fracture surface morphology and chronological age of the sample was found. Therefore, the fracture behavior of historic silk textiles seems to be primarily a function of fabric treatment and care rather than chronological age. No relationship was found between fabric color and the fracture surface morphology of the silk fibers. There was no correlation between elemental chemical composition and fabric color. The fabrics chosen for this study were all plain-weave, silk fabrics and stress located at yarn interlacings frequently dominated fracture behavior.

Interpretation of chemical composition data was difficult. Most elements appeared to be distributed evenly between fracture surfaces and whole fibers. The presence of these elements did not seem to influence fracture behavior. However, tin was found to be unevenly distributed throughout some fibers. Tin samples containing large concentration variations appeared to have fracture behavior dominated by heterogeneities.

Fracture patterns of a heat-degraded fabric sample indicated a loss of cohesion between fibrils or other supramolecular structural units during heating and low cohesion between supramolecular structures dominated fracture behavior in the heat-degraded samples. Fracture patterns of the light-degraded fabric samples indicated an increase in surface flaws resulted from light ex-

posure and surface flaws dominated fracture behavior in the light-degraded samples.

CHAPTER VI

RECOMMENDATIONS

The overall goal of this study was to increase understanding of the behavior of historic silk so that more research could be done to control deterioration of museum textile collections. This goal has been achieved and several interesting research topics have developed from this work. A few are briefly outlined below.

The effect of elemental composition on fiber fracture could be investigated with scanning electron microscopy dot mapping. Identification of exact locations of heavy concentrations of elements and their influence on fracture behavior could be studied.

New silk samples could be weighted with various elements used in historic weighting processes so the influence of the elements on fracture behavior and aging could be determined.

Restoration of silk fabrics damaged by thermal degradation might involve increasing interfibril cohesion. For example, crosslinking at low levels might be useful for this application.

Restoration of silk fabrics damaged by photochemical degradation might involve surface reactions that repair flaws. Research revealing the exact physical and chemical nature of the surface flaws would be required to guide in finish selection for repair of flaws.

REFERENCES

1. Andrews, E. H. Fracture in Polymers. Edinburgh: Oliver and Boyd, 1968.

2. Andrews, M. H. "The Fracture Mechanism of Wool Fibers Under Tension." Textile Research Journal 34 (October 1964): 831-835.

3. Anfinsen, C. B., Jr.; Anson, M. L.; Bailey, K.; and Edsall, J. T., eds. Advances in Protein Chemistry. Vol. 13. New York: Academic Press, Inc., 1958.

4. Asquith, R. S. Chemistry of Natural Protein Fibers. New York: Plenum Press, 1977.

5. Bogle, M. "The Deterioration of Silks Through Artificial Weighting." Textile Conservation Center Notes 11 (1978): 1-25.

6. Brecht, J.; DeVriest, K. L.; and Kausch, H. H. "On Some Aspects of Strength of Fibers." European Polymer Journal 7 (February 1971): 105-114.

7. Bunsell, A. R.; Hearle, J. W. S.; and Konopasek, L. "A Preliminary Study of the Fracture Morphology of Acrylic Fibers." Journal of Applied Polymer Science 18 (August 1974): 2229-2242.

8. Bunsell, A. R., and Hearle, J. W. S. "A Mechanism of Fatigue Failure in Nylon Fibers." Journal of Materials Science 6 (October 1971): 1303-1311.

9. Darby, W. D. Silk: The Queen of Fabrics. New York: The Dry Goods Economist, 1922.

10. Goswami, B. D., and Hearle, J. W. S. "A Comparison Study of Nylon Fiber Fracture." Textile Research Journal 46 (January 1976): 55-70.

11. Hearle, J. W. S. "Atlas of Fibre Fracture. 1." Textile Manufacturer 99 (January-February 1972): 14-15.

12. _____. "Atlas of Fibre Fracture. 2." Textile Manufacturer 99 (March 1972): 12-13.

13. _____. "Atlas of Fibre Fracture. 3." Textile Manufacturer 99 (May 1972): 20-21.

14. _____. "Atlas of Fibre Fracture. 4." Textile Manufacturer 99 (June 1972): 26-27.

15. _____. "Atlas of Fibre Fracture. 5." Textile Manufacturer 99 (July 1972): 42-43.

16. _____. "Atlas of Fibre Fracture. 6." Textile Manufacturer 99 (August 1972): 40-41.

17. _____. "Atlas of Fibre Fracture. 7." Textile Manufacturer 99 (September 1972): 16-17.

18. _____. "Atlas of Fibre Fracture. 8." Textile Manufacturer 99 (October 1972): 40-41.

19. _____. "Atlas of Fibre Fracture. 9." Textile Manufacturer 99 (November 1972): 12-13.

20. _____. "Atlas of Fibre Fracture. 10." Textile Manufacturer 99 (December 1972): 36-37.

21. _____. "Atlas of Fibre Fracture. 11." Textile Manufacturer 100 (January-February 1973): 24-25.

22. _____. "Atlas of Fibre Fracture. 12." Textile Manufacturer 100 (March 1973): 24-25.

23. _____. "Atlas of Fibre Fracture. 13." Textile Manufacturer 100 (April 1973): 34-35.

24. _____. "Atlas of Fibre Fracture. 14." Textile Manufacturer 100 (May 1973): 54-55.

25. _____. "Atlas of Fibre Fracture. 15." Textile Manufacturer 100 (June 1973): 44-45.

26. Hearle, J. W. S.; Buckley, C. P.; and Lomas, B. "Fracture, Fatigue and Wear of Man-Made Fibers." Manchester, England: Department of Textile Technology, University of Manchester, Institute of Science and Technology, n.d. (Typewritten).

27. Hearle, J. W. S., and Cross, R. M. "The Fractography of Thermoplastic Textile Fibers." Journal of Materials Science 5 (June 1970): 507-516.

28. Hearle, J. W. S.; Jariwala, B. C.; Konopasek, L.; and Lomas, B. "Aspects of Fracture of Wool and Hair Fibres." Proceedings 5th International Wool Textile Research Conference. Aechen, Germany: p. 370-380, 1977.

29. Hearle, J. W. S., and Sparrow, J. T. "The Fractography of Cotton Fibers." Textile Research Journal 4 (September 1971): 736-749.

30. Hooper, L. Silk: Its Production and Manufacture. London: Sir Issac Pitman and Sons, Ltd., n.d.

31. Lucas, F.; Shaw, J. T. B.; and Smith, S. G. "The Silk Fibroins." Advances in Protein Chemistry 13 (1958): 107-241.

32. Magoshi, J. and Nakamura, S. "Studies on Physical Properties and Structure of Silk. Glass Transition and Crystallization of Silk Fibroin." Journal of Applied Polymer Science 19 (April 1975): 1013-1015.

33. Makinson, K. Rachel. "Letter to the Editor: Fracture in Wool Fibers." Journal of the Textile Institute 61 (March 1970): 151-153.

34. Peterlin, Anton. "Molecular Model of Fracture of Fibrous Polymeric Material." Fracture 1977, ICF4, Waterloo, Canada, June 19-24, 1977 1 (1977): 471-485.

35. Peters. R. H. Textile Chemistry. Vol. 1. Amsterdam: Elsevier Publishing Company, 1963.

36. Sadov, F.; Korchagin, M.; and Matetsky, A. Chemical Technology of Fibrous Materials. Moscow: Mir Publishers, 1978.

37. Sakaguchi, I. "On the Mechanism of Tin Weighting of Silk and Nylon with Stannic Chloride." Journal of Faculty of Textile Science and Technology 49 (September 1968): 1-60.

38. Schnell, A. H. Silk and Mixed Goods. Vol. 1. Philadelphia: A. S. Schnell, 1935.

39. Scott, W. M. "The Weighting of Silk: Chapter I." American Dyestuff Reporter 20 (17 August 1931): 517-518, 539-540, 543.

40. Scott, W. M. "The Weighting of Silk: Chapter II." American Dyestuff Reporter 20 (31 August 1931): 557-562.

41. Scott, W. M. "The Weighting of Silk: Chapter III." American Dyestuff Reporter 20 (14 September 1931): 591-594.

42. Stockhauser, K. "Contributions to the Knowledge of Silk Weighting." The Melliand 2 (June 1930): 397-402.

43. Struik, L. C. E. Physical Aging in Amorphous Polymers and Other Materials. Amsterdam: Elsevier Scientific Publishing Company, 1978.

44. Tagliani, G. "A Survey of the Dyeing, Printing, and Finishing of Natural Silk." Journal of Society of Dyers and Colorists 6 (June 1934): 184-188.

45. Trutter, E. V. Natural Protein Fibers. New York: Harper and Row Publishers, Ind., 1973.

46. AATCC Technical Manual. Research Triangle Park, North Carolina: American Association of Textile Chemists and Colorists, 1978.

47. De Ferri Meallographia. Dusseldorf: Heydon and Son, Inc., 1979.

48. "Tracing Mineral Compounds in Textiles by Activation Analysis." Ciba Review 4 (1966): 30-32.

HISTORIC SILK FIBER FRACTURE

by

GAIL ELIZABETH GOODYEAR

B. S., California State University, Chico, 1979

AN ABSTRACT OF A MASTER'S THESIS

submitted in partial fulfillment of the

requirements for the degree

MASTER OF SCIENCE

Department of Clothing, Textiles and Interior Design

KANSAS STATE UNIVERSITY
Manhattan, Kansas

1981

ABSTRACT

Twenty-five historic silk fabrics dating from 1880 to 1980 were broken in a CRE tensile testing machine and evaluated to determine fiber fracture pattern characteristics of aged silks. Also studied were the effects of heat and accelerated light exposure on a new degummed silk crepe (Testfabrics, Inc.). Specimens of the silk crepe were heated for 6 hours at 60°C or exposed to carbon arc radiation for 320 AATCC Fading Units.

No correlation was found between fiber fracture surface morphology and chronological age. Most silk fibers exhibited fracture behavior based on surface flaws and structural heterogeneities. Fracture patterns of the heat-degraded sample indicated a loss of cohesion between fibrils or other supramolecular structural units. Fracture patterns of light-degraded fabrics indicate an increase in surface flaws result from light exposure. Analyses of chemical composition of the fibers showed most elements were uniformly distributed throughout some fibers and samples containing large concentration variation had fracture behavior dominated by heterogeneities.